Dynamics of Compressed Polymer Layers Adsorbed on Solid Surfaces

E. Pelletier and J. P. Montfort*

Laboratoire de Physique des Matériaux Industriels, U.R.A. C.N.R.S. 1494, Université de Pau et des Pays de l'Adour, 64000 Pau, France

J. L. Loubet, A. Tonck, and J. M. Georges

Laboratoire de Tribologie et de Dynamique des Systèmes, U.R.A. C.N.R.S. 855, Ecole Centrale de Lyon, Ecully 69 131, France

Received October 7, 1993; Revised Manuscript Received December 1, 1994®

ABSTRACT: The viscoelastic properties of thin polymer films confined between a sphere and a plane are investigated by use of a surface force apparatus designed as a rheometer operating at the molecular scale. Axial oscillatory motions yield a shear field from which a complex elastic modulus of the confined fluid can be deduced. As the sphere–plane distance is decreased, the fluid made of two adsorbed polymer layers and the free solution exhibits a liquid–solidlike transition at distance h_c. The measured complex modulus can be split into an elastic modulus G_c accounting for the compression of the adsorbed chains and a complex shear modulus $G_H^*(\omega)$ expressing the draining process at the interface. The elastic modulus G_c is directly connected to the gradient of static repulsive forces, and a compression modulus E_N of the adsorbed overlapping layers can be deduced from G_c. The flow term $G_H^*(\omega)$ is discussed in terms of viscoelastic parameters (zero-shear viscosity η_0, average relaxation time τ_0) as a function of sphere–plane distance h. For moderately compressed layers, a correlation length ξ can be defined either from the compression modulus E_N or from the zero-shear viscosity η_0. Both lengths scale as $(h_c - h)^{-4/9}$.

Introduction

The viscoelastic behavior of a polymeric liquid interacting with a surface is different from that of the bulk. Investigating its properties is fundamental in fields dealing with interfaces, e.g., adhesion processes, polymer blends, composite materials, and flow in porous media. One of the most appropriate ways to characterize the rheological properties of polymer solutions is to perform periodic shearing experiments from which the complex elastic modulus $G^*(\omega)$ is deduced as a function of frequency.[1] New techniques make possible rheological studies of very thin films confined between two solid surfaces. The distance h between the two surfaces can be as little as a few angstroms.

Some attempts have been made to use a modified surface force apparatus for carrying out microrheology experiments of confined liquids. The surface force apparatus designed by Israelachvili and Tabor[2] has been widely used for analyzing the static and viscous forces of very confined media. Two kinds of dynamic deformations of the gap have been used: normal[3–9] and tangential[10–16] motions of the surfaces relative to each other. They are appropriate for investigating respectively moderately and strongly confined systems. Lubrication experiments deal with either adsorbed or grafted layers in the presence of pure solvent or unentangled polymer melts. The apparent dynamic viscosity is analyzed as a function of distance but the elastic properties are not investigated separately from the viscous ones. The main findings are (i) an enhanced viscosity at short distances and (ii) a liquid–solidlike transition when a finite shear stress is needed for allowing shear.

Furthermore, as the surfaces are made of thin sheets of mica glued onto crossed glass cylinders, they are easily deformed when the interaction forces increase. Therefore, that equipment is not suitable for highly viscous fluids which yield high hydrodynamic forces or imposes strongly confined systems, for example, overlapping layers, which exhibit large repulsive static forces.

In those cases, as the two surfaces are flattened, friction experiments are possible by imposing tangential motions to a surface. The results obtained both on simple liquids and on unentangled polymer melts are characterized by a critical shear stress required to initiate the sliding of the solid surfaces. Thus, the concept of shear viscosity is no longer appropriate for describing the rheological properties of such thin films.

The most relevant paper that deals with linear viscoelasticity of confined polymer melts is by Hu and Granick.[16] For two different molecular weights of unentangled poly(phenylmethylsiloxane), they found a purely viscous behavior at large distance and elastic behavior at short distance. The crossover distance is of the order of $4R_g$. In the compressed state, they suggest that the elastic effects can be viewed as entanglement phenomena.

The aim of this paper is to comprehensively study the viscoelastic properties of confined polymer solutions by means of a surface force apparatus with metallic surfaces appropriate for measuring large static and dynamic forces without noticeable deformations. Therefore, normal oscillatory motions in a large range of distances and frequencies will provide information on the dynamics of adsorbed and free chains confined within a plane–sphere gap. The closest distance h will cover a large range including the overlapping and nonoverlapping situation as far as adsorbed layers are concerned. The ability of that equipment to describe the viscoelastic behavior of a semidilute solution of a high polymer in a wide range of frequencies at distances much larger than the radius of gyration of the chains has been demonstrated earlier.[17]

This study will focus on distances just below and above the overlapping threshold h_c where a dramatic

® Abstract published in *Advance ACS Abstracts,* February 1, 1995.

0024-9297/95/2228-1990$09.00/0

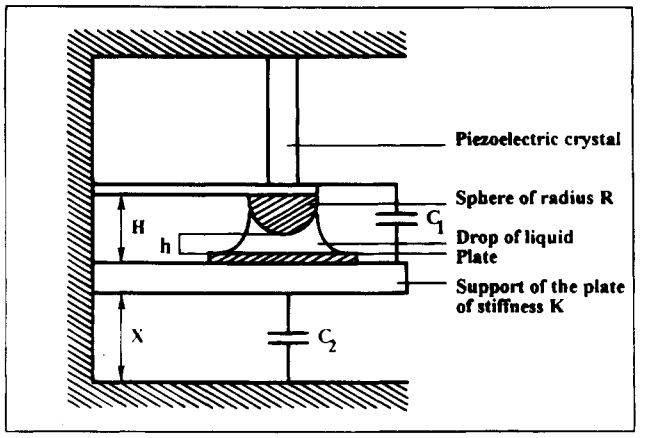

Figure 1. Schematic of the experimental setup.

change on the elastic component of the complex elastic modulus $G^*(\omega)$ occurs. The first part will be mainly devoted to a description of the equipment and the relations between the static or dynamic forces and the complex modulus $G^*(\omega)$. In the second part, we will describe and analyze the viscoelastic response as a function of distance in terms of the compression modulus, zero-shear viscosity, and relaxation times.

Experimental Section

(a) Surface Force Apparatus. All experiments presented have been done with the surface force apparatus designed by the Ecole Centrale de Lyon. Figure 1 shows a diagram of the experimental unit, which is described in more detail elsewhere.[17-19]

A drop of solution is confined between the plate and the sphere. The sphere of radius R is moved axially by a piezoelectric crystal. The plate is supported by an adjustable double-cantilever spring, and the transducer C_2 measures its absolute motion X_0.

As the spring stiffness K varies over a wide range, normal forces can be measured from 10^{-8} up to 10^{-1} N. The closest separation h between the plate and the sphere is calculated from the capacitance of the plate−sphere capacitor: the two surfaces have a thin coating of cobalt on the glass supports. That distance h can be compared to the distance H between the stands of the plate and the sphere given by transducer C_1. When the two surfaces are undeformed, the two distances exhibit the same variations. Furthermore, a distance-feedback loop incorporated into the C_1 circuit allows one to impose and control the plate−sphere distance. That is a mandatory condition for stress relaxation experiments after cessation of flow and mechanical spectrometry at a given distance, e.g., at a given state of confinement. Stress relaxation is yielded by stopping the axial motion of the sphere after a drainage experiment at constant velocity. The relaxation of the hydrodynamic forces brings about a decrease of the deflection of the spring which would modify the plate−sphere distance if the servo-loop system did not exist. Such experiments will be described in a subsequent paper.

On the other hand, after complete relaxation of the draining forces, oscillatory experiments can be carried out around an average distance h_0. The amplitude γh_0 of the oscillations is kept small enough—γ lower than 1%—in order to stay in the framework of linear viscoelasticity. In fact, local shear rates are proportional to $\gamma\omega$, and the amplitude is adjusted to the frequency ω, which varies from 10^{-3} up to 10^3 s^{-1}. In the area of strong repulsive static forces, low amplitudes are also needed in order to consider linear variations of the static forces as a function of distance h. Therefore, the total normal force exerted on the plate can be analyzed in terms of in-phase and out-of-phase components by means of two lock-in amplifiers, and the sinusoidal shape of the signal is checked on the screen of an oscilloscope.

(b) Complex Elastic Modulus. When carrying out dynamic experiments by imposing a sinusoidal voltage on the piezoelectric crystal, the motion of the plane is governed by the equation

$$m\ddot{X} + c_2\dot{X} + KX + c_1\dot{H} + F_T(h,\dot{h}) = 0 \qquad (1)$$

where m is the mass of the plate and its stand, c_1 and c_2 are the viscous coefficients associated with the related transducers, the F_T stands for the total force exerted between the sphere and the plane. It is the sum of the static and dynamic contributions.

Static Forces. They include all the static interactions between the sphere and the plane such as wetting forces created by the liquid meniscus (their variations can be neglected if the radius of the liquid meniscus is comparable to the radius of the sphere[18]), surface forces such as van der Waals forces, and steric forces due to the confinement of the macromolecules.

As the sphere is submitted to small sinusoidal displacements around an average position, linear variations of the static force F_s around its equilibrium position are to be considered:

$$F_s = F_s(h_0) + \left.\frac{dF_s}{dh}\right|_{h_0}(h(t) - h_0) = F_s(h_0) + \left.\frac{dF_s}{dh}\right|_{h_0} h_0\gamma e^{j(\omega t+\varphi)} \qquad (2)$$

with φ the phase shift between the motion imposed on the sphere and the variations of the distance h.

Dynamic Forces. It has been shown that the expression of the hydrodynamic force F_H for a homogeneous viscoelastic fluid confined between a plane and a sphere is[7]

$$F_H(t) = -\frac{6\pi R^2}{h(t)}\int_{-\infty}^{t} G_H(t-t')\frac{dh}{dt'}\,dt' \quad \text{for} \quad h \ll R \qquad (3)$$

where $G_H(t)$ is the relaxation modulus accounting for the past mechanical history of the sample.

Then for small oscillations compared to the average distance ($\gamma \ll 1$), F_H becomes

$$F_H(t) = -6\pi R^2\gamma G_H^*(\omega)e^{j(\omega t+\varphi)} \qquad (4)$$

where G_H^* defines a complex modulus which is the Laplace transform of $j\omega G_H(t)$.

Therefore, using eqs 2 and 4 and assuming that the equilibrium force $F_s(h_0)$ is offset by the average spring force KX_0 of the cantilever, the motion equation of the plate can be cast into

$$\frac{X(t) - X_0}{h(t) - H_0}[-m\omega^2 + j\omega c_2 + K] + j\omega c_1 = \left.\frac{dF_s}{dh}\right|_{h_0} + \frac{6\pi R^2}{h_0}G_H^*(\omega) \qquad (5)$$

$X(t)$ and $H(t)$ are respectively measured from transducers C_2 and C_1. Then the combined contributions of the static and dynamic forces to an overall complex modulus $G^*(\omega)$ can be calculated from experimental data and written from eq 5 as

$$G^*(\omega) = G_H^*(\omega) - \frac{h_0}{6\pi R^2}\left.\frac{dF_s}{dh}\right|_{h_0} \qquad (6)$$

The hydrodynamic term is dominant when the variations of the static interactions are weak as happens at distances much larger than the radius of gyration of the macromolecules. On the other side, strong repulsive forces occurring at short distances will lead to a major contribution at low frequencies where the hydrodynamic component vanishes.

(c) Materials. The sphere and the plate consist of fused borosilicate glass covered by a thin deposit of cobalt (≈500 Å) to make the surfaces conducting. A detailed analysis of these surfaces has already been published.[19] The average peak-to-

Table 1. Main Features of the Samples[a]

R (mm)	1.64	1.32	1.49	1.45	1.40	1.32
C (%)	3.6	2.0	1.2	0.7	0.3	0.2
h_c (Å)	490	355	340	585	295	290

[a] R, radius of the spheres; C, weight polymer concentration of the solutions; h_c, crossover distance of compressed layers which defines an "elastic" thickness L of the adsorbed layers ($h_c = 2L$). L is comparable to the radius of gyration of the chains, $R_g \approx 215$ Å.

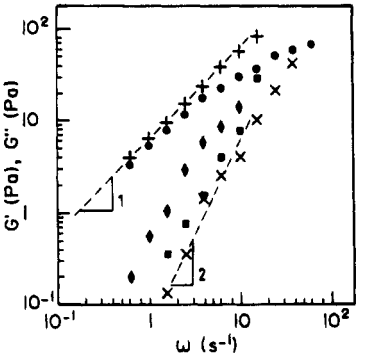

Figure 2. Complex shear modulus of the solvent at different distances as a function of frequency: storage modulus G' ((◆) 80 Å; (■) 196 Å; (×) 203 Å) and loss modulus G'' ((●) 80 Å; (+) 196 Å).

peak roughness is around 10 Å, and the reduced Young's modulus measured by microindentation of the covered surfaces is 8×10^{10} Pa. The radius of the spheres is typically 1.4 mm (Table 1).

The linear polybutadiene sample (Polymer Laboratories) has a narrow molecular weight distribution: weight-average molecular weight $M_w = 330\,000$ g·mol^{-1} and polydispersity index $M_w/M_n = 1.04$.

As the average molecular weight between entanglements M_e is estimated at 1900 g·mol^{-1},[20] the melt is highly entangled. In solution, different crossover concentrations can be defined.

As we are interest in viscoelastic properties, we use the crossover molecular weight for viscosity $M_c \cong 2M_e$, which defines a crossover concentration $C^* = M_c/M_n \cong 1.1\%$. Different concentrations above and below C^* are used (Table 1). The polybutadiene sample was diluted in a nonvolatile hydrocarbon oil solvent provided by Exxon (Flexon 391). This condition is imposed by the fact that the plate and the sphere are in open air and not enclosed in a box. Furthermore, a previous comprehensive study of the viscoelastic bulk properties of the same solutions[21] will help us to compare them to their behavior in a confined space. The experiments are conducted at room temperaure ($T = 24$ °C), which is far above the glass transition temperature of the polymer ($T_g = -101$ °C[22]) and of the solvent ($T_g = -39.5$ °C[21]).

A drop of solution is introduced between the sphere and the plate. Then the solution is left for about 20 h to equilibrate at very large separation in order not to disturb the chain diffusion between the solution and the surfaces. The incubation distance is about 1 μm, which is much larger than the radius of gyration of the macromolecules ($R_g = 215$ Å).[23] Adsorbed layers of polybutadiene are expected to be formed in contact with high-energy cobalt surfaces. As the static force profile does not change during the experimental period (around 3 days),[24] we can assume that the surface coverage is constant. After incubation, the surfaces are brought closer and oscillatory experiments are carried out at different distances h_0 where the adsorbed layers overlap or do not overlap each other.

Dynamic Experiments

Solvent. The complex shear modulus of the pure solvent measured at different distances (Figure 2) shows that for h_0 greater than 80 Å, the loss modulus G'' exceeds the storage modulus G' by more than 2 orders of magnitude for frequencies lower than unity. Furthermore, as the loss modulus scales as ω, the solvent can be considered as a Newtonian fluid with a constant viscosity of about 6 Pa·s whatever the distance. A pronounced non-Newtonian behavior is seen around 80 Å, which is the distance where static repulsive forces appear (Figure 3). That reveals a modification of the film structure when the distance h_0 is of the same order of the molecular dimensions. Both theoretical[25] and experimental[16] studies of liquids made of spherical or short-chain molecules have interpreted their static and dynamic properties in terms of ordering or layering occurring at distances commensurate with the molecular dimensions. As we are going to deal with confined solutions of polybutadiene with moderately compressed polymer layers, the range of distances will exceed about 200 Å, where the behavior of the solvent is purely viscous.

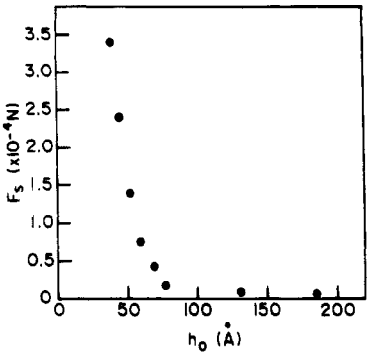

Figure 3. Static force profile for pure confined solvent.

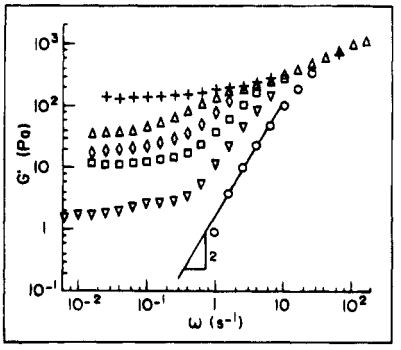

Figure 4. Storage modulus G' versus ω for different distances: (+) 390 Å; (△) 451 Å; (◇) 464 Å; (□) 475 Å; (▽) 501 Å; (○) 586 Å. The concentration of the solution is $C = 3.6\%$.

Solutions of Polybutadiene. The complex modulus $G^*(\omega)$ of the solutions listed in Table 1 has been measured at distances shorter than a few thousand angstroms. At large distances, the viscoelastic behavior is exactly the same as for the bulk solutions.[21] The terminal zone of the relaxation spectrum accounting for the chain diffusion is explored and the usual viscoelastic parameters—zero-shear viscosity η_0, steady-state compliance $J_e°$, and average relaxation time $\tau_0 = \eta_0 J_e°$—can be analyzed in terms of concentration dependence.

However, the rheological behavior of more confined solutions exhibits a sharp transition when the distance is of the same order of magnitude as the radius of gyration of the macromolecules. As an example, Figures 4 and 5 show the crossover region between 306 and 259 Å for a dilute solution ($C = 0.2\%$). Within 5 Å, the storage modulus $G'(\omega)$ increases dramatically at low frequencies and it varies as a function of frequency from the usual square law toward a constant value. At the same time, the loss modulus $G''(\omega)$ increases steadily

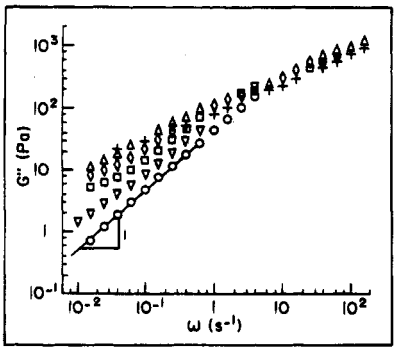

Figure 5. Loss modulus G'' versus ω for the same thicknesses as in Figure 4. The concentration of the solution is $C = 3.6\%$.

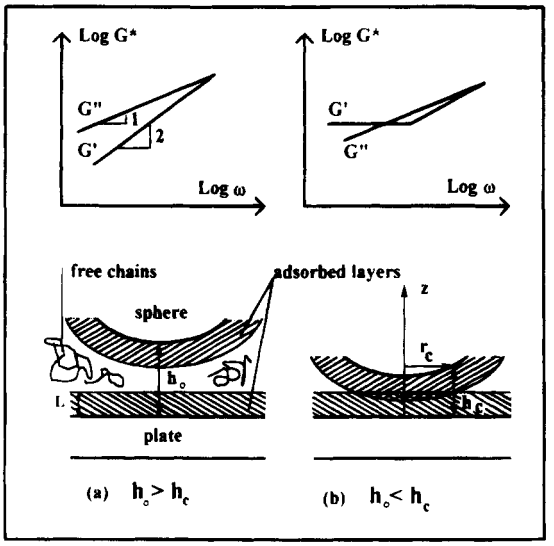

Figure 6. Schematic representation of the viscoelastic behavior of confined solutions according to the closest separation h_0 between the two surfaces ($L = h_0/2$ is the thickness of the adsorbed layers): (a) at large distances, $h_0 > h_c$, the dynamic lubrication forces dominate and give rise to the complex shear modulus of a viscoelastic liquid; (b) when the adsorbed layers overlap ($h_0 < h_c$) at low frequencies, the elastic modulus accounts for the axial deformation of the network formed in the central area.

and does not exhibit the sharp transition shown by the storage modulus.

Then we can define with a good accuracy a critical distance h_c (i) above which the confined solution globally behaves as a viscoelastic liquid consisting of two adsorbed polymer layers separated by a solution of free chains (Figure 6a) and (ii) below which the adsorbed layers are overlapping each other (Figure 6b). Therefore, the viscoelastic behavior is a combination of two phenomena: (i) the elastic response of the tethered chains which are compressed in the central area and are responsible for the constant storage modulus at low frequencies (its value will be denoted G_c) and (ii) the diffusion of the free chains in the outer region of the interface. Hence, the critical distance h_c defines the compression threshold of the adsorbed layers. In other words, $h_c/2$ is an average thickness of the layers relative to dynamic properties. As illustrated in Figure 7, the value of G_c is zero at large distances and increases steadily with the confinement. Therefore, an extrapolation of the experimental curve allows us to define h_c with a very good accuracy.

Compression Modulus E_N and Static Force F_s. For distances shorter than h_c, the main contribution to the overall complex modulus $G^*(\omega)$ is, at low frequencies, a constant storage modulus G_c. The confined solution behaves as a viscoelastic solid.

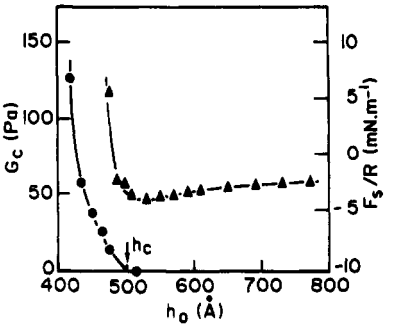

Figure 7. Static force F_s (▲) as a function of distance h_0 (polymer fraction $C = 3.6\%$). The crossover distance h_c at which the overlapping layers give rise to a normal stress G_c (●) response is roughly the same as the minimum of the static force curve.

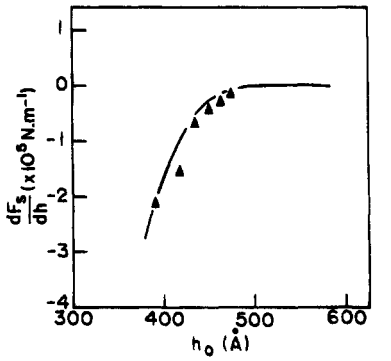

Figure 8. Plot of the derivative or the static force as a function of distance (full line). Values calculated by eq 7 from the plateau modulus G_c (▲) fit the experimental curve. Polymer fraction $C = 3.6\%$.

We postulate that it is due to the compression of the adsorbed chains. This assumption is in agreement with the fact that the static forces do not vary over a period of several days. The exchange processes between the layers and the solution are extremely slow. As a consequence, the number of chains involved in the adsorption process is constant. That is the situation of restraint equilibrium[26] during which the overlapping layers must be compressed; the tethered chains exhibit a nonequilibrium conformation and should result in repulsive restoring forces between the two surfaces. This is confirmed by the static force curve in Figure 7, which shows that the storage modulus G_c appears when the static forces are repulsive. More precisely, the threshold h_c roughly matches the distance at which the repulsive forces start to compensate the attractive ones, near the minimum of the static force curve.

This observation implies a direct connection between static dynamic measurements. Using eq 6, one can straightforwardly write

$$G_c = -\frac{6\pi R^2}{h_0}\frac{dF_s}{dh} \tag{7}$$

which is consistent with the fact that G_c appears at the minimum of the static curve. The above relation is quantitatively verified as illustrated in Figure 8.

We must also notice that eq 7 holds for all distances. When h_0 is larger than h_c, the derivative is positive and the storage modulus should be diminished. Meanwhile, in this range of distances, the derivatives are weak and are multiplied by a geometrical factor h_0/R^2 ($R \approx 1$ mm,

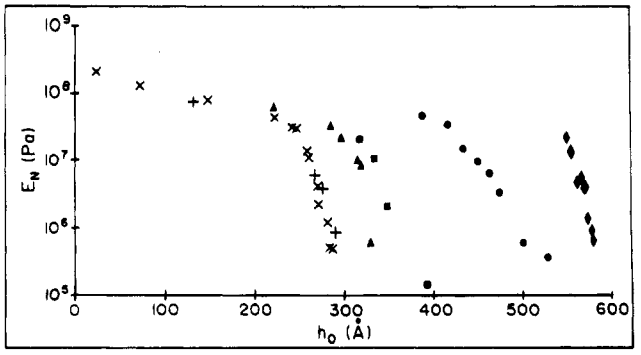

Figure 9. Compression modulus, E_N, for different polymer concentrations: (×) 0.2%; (+) 0.3%; (◆) 0.7%; (▲) 1.2%; (■) 2.0%; (●) 3.6%.

$h_0 \approx 100$ Å, $h_0/R^2 \approx 10^{-2}$ m^{-1}). Then the attached negative term is negligible when included in the global modulus $G^*(\omega)$.

Fredrickson and Pincus[27] have theoretically investigated the dynamic behavior of grafted polymer layers submitted to oscillatory squeezing between a sphere and a plane. They have shown that in a compressed situation an elastic term has to be added to the flow component, which accounts for the axial deformation of the polymer chains. This dynamic normal force F_N is the incremental change of the osmotic pressure associated with the displacement and integrated over the contact surface between the layers. It is defined as

$$F_N = -\frac{8}{9}\pi R\gamma h_0 E_N(h_0) \tag{8}$$

where E_N is an elastic compression modulus which scales as the osmotic pressure:

$$E_N = K_0 \frac{k_b T}{\xi^3} \tag{9}$$

where ξ stands for the mesh size of the polymer network created in the confined medium and K_0 is a numerical factor. Grafted layers are supposed to exhibit brush conformations with a constant monomer concentration whereas that concentration should decrease with the distance from the surface in a power law fashion for adsorbed layers.[28] That difference does not change the distance dependence of the normal force F_N and accordingly the compression modulus E_N.

Therefore, the compression modulus E_N can be easily related to the storage modulus G_c for infinitesimal oscillations. In that case, the normal force amplitude F_N is connected to the gradient of the static repulsive forces by

$$F_N = \gamma h_0 \left.\frac{dF_s}{dh}\right|_{h_0} \tag{10}$$

Then using relations 7 and 8, we obtain

$$E_N(h_0) = \frac{27}{4}\frac{R}{h_0} G_c(h_0) \tag{11}$$

The compression modulus E_N plotted as a function of separation h_0 (Figure 9) for all concentrations shows that there is no power law dependence for moderately compressed layers. From h_c, there is a steep increase of E_N followed by a slower variation. At distances of about $h_c - 10$ Å, E_N has the same value as the rubbery

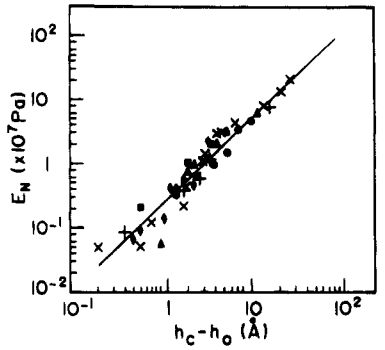

Figure 10. Master curve for the compression modulus, E_N, versus the penetration length, $h_c - h_0$, of the adsorbed layers. Same symbols as in Figure 9. The best fit (full line) gives $E_N \approx (h_c - h_0)^{4/3}$.

plateau modulus of polybutadiene melts ($\sim 3 \times 10^6$ Pa) and might reach the value of the glassy modulus ($\sim 10^9$ Pa) in strongly confined states. For unentangled confined melts, Hu and Granick[16] measured a plateau modulus which is about twice the rubberlike plateau modulus G_N° of bulk entangled melts at distances around $3-5R_G$. They suggest that the elastic effects observed can be viewed as entanglement phenomena. Measurements at shorter distances should ascertain whether the observed plateau modulus levels off or increases toward a glassy state. A master curve is obtained (Figure 10) when the compression modulus E_N is plotted as a function of some kind of penetration length, i.e., $h_c - h_0$. For all concentrations, E_N scales as $(h_c - h_0)^{4/3}$. Therefore, according to eq 9, the mesh size of the interfacial network scales as $\xi \approx (h_c - h_0)^{-4/9}$.

To our knowledge, no theoretical predictions have been made in the case of adsorbed layers in the presence of free chains in solution. Fredrickson and Pincus[27] dealt with grafted layers in contact with a pure good solvent. For moderately compressed layers, the volume fraction of polymer remains small and the layers should be considered as semidilute layers. The hydrodynamic screening length for semidilute solutions (with good solvents) scales with monomer concentration C as $\xi_H \approx C^{-3/4}$. As the static correlation length ξ related to the osmotic pressure is expected to be proportional to ξ_H, they predict $\xi \approx h_0^{3/4}$. Even though the free chains which are in the vicinity of the adsorbed layers should perturb the local monomer concentration, we can expect that more confined solutions leading to strongly compressed layers will yield a constant concentration within the layers. Therefore, the above theory should be appropriate.

Hydrodynamic Complex Modulus. For $h < h_c$, the measured modulus $G^*(\omega)$ is the sum of an elastic modulus G_c and a complex shear modulus $G_H^*(\omega)$ accounting for the diffusion processes of the solvent and the free chains. That contribution can be isolated by subtracting G_c from the measured storage modulus $G'(\omega)$. As an example, Figure 11 shows that the hydrodynamic storage modulus $G'_H(\omega)$ scales as ω^2, which is characteristic of the terminal zone of relaxation for viscoelastic liquids.

Another way to point out the change which appears in the terminal zone when G_c is removed from $G^*(\omega)$ is to use a complex representation of the viscosity $\eta^*(\omega) = G^*/\omega$. Figure 12a shows that plotting η'' as a function of η' enables one to discriminate different relaxation modes.

When $h_0 > h_c$, the curve exhibits only one domain as expected for a bulk solution of homopolymer. The shape

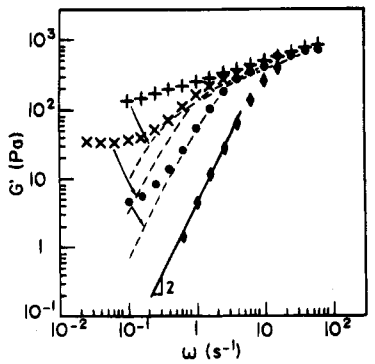

Figure 11. Measured storage modulus, $G'(\omega)$, and hydrodynamic storage modulus $G_H'(\omega) = G'(\omega) - G_c$ versus frequency at different distances: (+) 551 Å; (×) 567 Å; (●) 580 Å; (◆) 628 Å. Polymer fraction $C = 0.7\%$ and crossover distance $h_c \approx 585$ Å. The dashed lines stand for the hydrodynamic components of the related experimental storage modulus. In the asymptotic region, G_H' scales as ω^2.

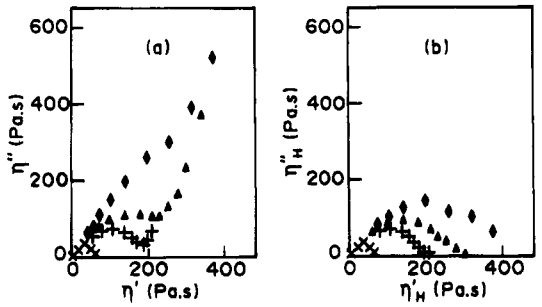

Figure 12. Cole–Cole plot of the complex viscosities: (a) experimental viscosity $\eta^* = G^*/\omega$; (b) hydrodynamic viscosity, $\eta_H^* = (G^* - G_c)$. The different distances are (◆) 556, (▲) 570, (+) 580, and (×) 611 Å. Same solution as in Figure 11.

is different below h_c. The Cole–Cole plot exhibits two relaxation areas: the main one is due to the same cause as above, and a second relaxation process appears at low frequencies. The relaxation times involved in this process are very long and not accessible experimentally. Nevertheless, that is evidence for very slow relaxation processes due to hindered motions of the adsorbed chains. As the attached domain in the Cole–Cole plot is not entirely described, a first approximation is to consider it as an elastic term. Thus, removing the elastic modulus G_c from the overall complex modulus $G^*(\omega)$ leads to the complex viscosity $\eta_H^*(\omega) = (G^*(\omega) - G_c)/\omega$, which defines the first domain (Figure 12b).

Then we are able to define viscoelastic parameters which describe the main features of the relaxation mechanisms involved in the confined solutions: zero-shear viscosity $\eta_0 = \lim_{\omega \to 0} \eta'_H$, steady-state compliance $J_e^\circ = (1/\eta_0^2) \lim_{\omega \to 0}(G'_H/\omega^2)$, and average relaxation time $\tau_0 = \eta_0 J_e^\circ$.

Zero-Shear Viscosity. The plots of η_0 as a function of separation h_0 (Figures 13 and 14) show a sharp increase of viscosity near h_c. However, at large distances, distinct behaviors appear according to the concentration. Dilute solutions (Figure 13) show a monotonous increase of viscosity at all distances in contrast with semidilute solutions, which present a minimum of viscosity above h_c (Figure 14). This minimum should be consistent with a global decrease of the concentration in the gap due to the ejection of free chains or with slipping motions at the solution–layer interface. Such motions have been investigated theoretically.[29]

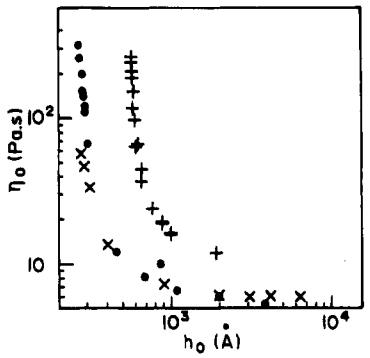

Figure 13. Zero-shear viscosity η_0 versus distance h_0 for concentrations lower than C^*: (●) 0.2%; (×) 0.3%; (+) 0.7%.

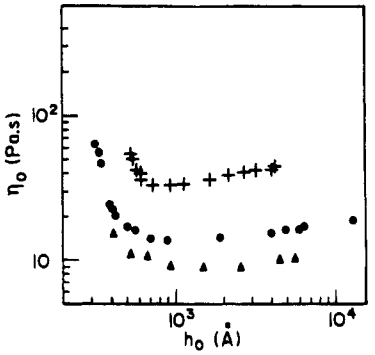

Figure 14. Zero-shear viscosity η_0 versus distance h_0 for concentrations higher than C^*: (▲) 1.2%; (●) 2.0%; (+) 3.6%.

Let us focus on dilute solutions where the long-distance zero-shear viscosity is very close to the pure solvent viscosity. This means that the contribution of free chains is negligible as far as viscosity is concerned. *For overlapping polymer layers* ($h_0 < h_c$), Fredrickson and Pincus[27] assign the viscosity term to the draining of solvent molecules through the network made of the grafted chains. They use Brinkman's equation for describing the solvent velocity field by means of a hydrodynamic screening length ξ_H and predict a viscosity coefficient in the form

$$\eta_0 = \frac{2}{9}\eta_s\left(\frac{h_0}{\xi_H(h_0)}\right)^2 \qquad (12)$$

Figure 15 shows that, despite an unexplained shift of the curves, the hydrodynamic screening length deduced from viscosity measurements of moderately compressed layers scales in the same way as the mesh size of the network: $\xi_H \propto (h_c - h_0)^{-4/9}$. The values are consistent with the average distance a between entanglements for polybutadiene melts[30] ($a \approx 60$ Å). Furthermore, recalling that the Young's modulus E_N can be related to the mesh size ξ (relation 9) which plays the role of a static correlation length, one could estimate the ratio ξ_H/ξ. That can be done if we know the value of the prefactor K_0 in relation 9. Rault[30] has shown that a melt of entangled polymer can be compared to a number ν of interpenetrating networks with a mesh size ξ, leading to a rubbery shear plateau modulus $G_N = \nu kT/\xi^3$. As he found a universal value of ν ($\nu \cong 25$) and assuming the incompressibility condition, the Young's modulus is $E_N = 3G_N$, leading to $K = 75$. Thus, the value of ξ deduced from relation 9 is exactly the same as ξ_H for the most dilute solution ($C = 0.2\%$) and $\xi_H/\xi = 2$ for the other concentrations as shown in Figure 15. That first attempt for estimating the ratio ξ_H/ξ from nanorheo-

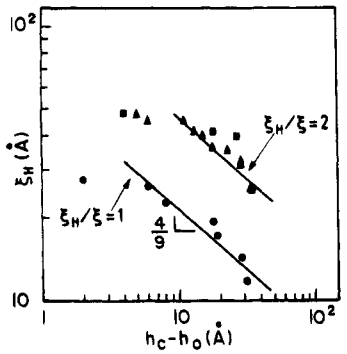

Figure 15. Hydrodynamic screening length ξ_H for compressed layers ($h_0 < h_c$) as a function of distance h_0 for solution concentrations lower than C^*: (●) 0.2%; (■) 0.3%; (▲) 0.7%. The values of ξ_H are calculated from viscosity data (relation 12). The full lines are obtained from the master curve of the compression modulus E_N (Figure 10) and relation 9 defining a static correlation length ξ. The scaling laws as a function of distance are the same for both lengths. From an evaluation of the prefactor $K_0 = 75$, we can estimate the ratio ξ_H/ξ at unity for $C = 0.2\%$ and 2 for the other concentrations.

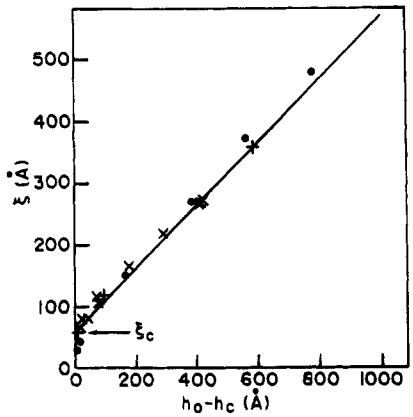

Figure 16. Mesh size ξ of the network made of bridging chains for nonoverlapping layers and polymer concentrations $C < C^*$: (●) 0.2%; (×) 0.3%; (+) 0.7%.

logical measurements is very encouraging and needs further careful experiments conducted with well-defined systems. Lubrication experiments conducted on compressed polymer brushes by Klein et al.[9] have also been interpreted in terms of an effective viscosity η_{eff} given by eq 12 and a correlation length scaling as h^{α} like in a semidilute regime. The related fit of the experimental function $\xi = h/\eta_{eff}$ does not allow one to confirm the above scaling law.

On the other hand, at distances larger than h_c, the static forces are attractive. That has been interpreted by bridging effects: segments of chains adsorbed on one surface penetrate into the opposite layer and are adsorbed onto the other surface. The chains pinned on both surfaces are stretched at large distances and exert an attractive restoring force. Assuming that they create a network with a mesh size ξ of the same order of magnitude of the distance $h - h_c$ between the adsorbed layers and that the main dragging force is due to the draining of the solvent within that network, we can also estimate the mesh size ξ from viscosity measurements (relation 12). The experimental law (Figure 16) is given by $\xi - \xi_c = (h_0 - h_c)/2$ with values of ξ lower than $h_0 - h_c$, in agreement with our assumptions. Moreover, the value of the mesh size ξ_c at the crossover distance h_c ($\xi_c \cong 60$ Å) is consistent with the distance between entanglements in polybutadiene melts.

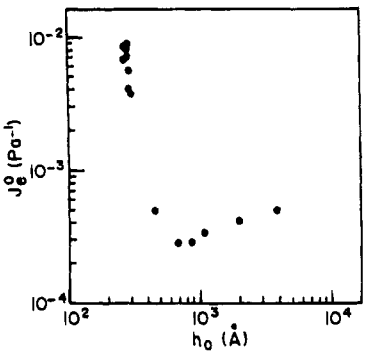

Figure 17. Steady-state compliance J_e° versus distance h_0 ($C = 0.2\%$).

Steady-State Compliance. The asymptotic behavior of G_H' at low frequencies provides an elastic parameter, the steady-state compliance J_e°, which accounts for the elastic deformation during steady flow. It also represents elastic energy storage which is recoverable after the stress is removed.

The experimental results (Figure 17) show that, at large distances, even for very dilute solutions, a high value of J_e° reveals the presence of a few chains in the free solution. It has been demonstrated that the concentration dependence of the steady-state compliance of dilute solutions scales as C^{-1} [21] and that J_e° increases dramatically with the relaxation time distribution.[31] These main features can explain the variation observed in Figure 17. As the two surfaces are moved closer, the average concentration of chains in the intermediate solution increases, mainly because of a few chains trapped within the loops of the adsorbed layers. Therefore, J_e° should decrease according to the above law. But this effect is overwhelmed around and below h_c by the fact that the diffusion mechanisms of the trapped chain and the overlapped loops lead to an increase of the relaxation time distribution and subsequently of the compliance. In fact, the steady-state compliance reveals, in a very sensitive way, the changes occurring in the relaxation mechanisms involved in the confinement process. However, a quantitative analysis of experimental results needs to identify those mechanisms. Furthermore, the presence of free chains is perturbing and to some extent it could generate mechanisms such as radial deformation of the adsorbed layers in the solvent flow.

Relaxation Times. An average relaxation time τ_0 can be defined as the product $\eta_0 J_e^\circ$. For dilute confined solutions, the relaxation time increases with confinement from 10^{-2} to 10 s when the ratio h_0/h_c varies from 10 to 0.8 (Figures 13 and 17). At large distances, the values of τ_0 are consistent with those of free solutions[21] whereas the highest value is the same as for a melt. This observation can be related to the fact the correlation length ξ in the moderately compressed situation is comparable with the distance between entanglements (~60 Å). Those results have to be interpreted in terms of free chains trapped inside the loops of the adsorbed layers and reptating like in a melt.

For strongly compressed layers, we expect a steady increase of the average relaxation time of trapped chains according to the scaling law of the correlation length but that diffusion process should be overwhelmed by the friction of the adsorbed chains belonging to the opposite surfaces and which are overlapped.[32] In that case, an exponential variation of the relaxation times is expected, as exhibited by entangled star polymers:

$$\tau = \tau_1 N^2 \exp(\alpha N/N_e(c)) \quad (13)$$

where τ_1 is a microscopic time, N is the total number of monomers per chain, and N_e is the number of monomers between entanglements in the adsorbed layers.

On the other hand, Fredrickson and Pincus[27] define a characteristic time $\tau(h)$ from the relaxation modulus $G_H(t)$. That time is associated with the radial deformation of the brushes in the solvent flow. It is the Zimm relaxation time for a blob to diffuse between the two surfaces:

$$\tau(h) \approx \frac{\eta h^2 \xi}{6kT} \quad (14)$$

In our experiments the order of magnitude of $\tau(h)$ around h_c is close to 10^{-5} s. That value is far lower than the observed relaxation time. The usual frequency range is appropriate for slower relaxation processes which are not described by the Fredrickson–Pincus approach.

A realistic model to apply for semidilute solutions should consider the reptation of the free chains through the polymer network between the surfaces. Such a model has not been built yet despite that de Gennes[33] has already considered the reptation of a free chain inside a self-similar layer in a direction parallel to a flat surface.

Conclusion

The analysis of oscillatory lubrication forces between polymer surfaces yields a simultaneous knowledge of the viscous and elastic responses of the confined medium accounting for the specific behavior of squeezed polymer layers. Experiments have been conducted in the largest range of frequencies compatible with the design of a surface force apparatus capable of operating with surface forces without noticeable deformations. The frequency range could be extended if the time–temperature superpositin principle is applicable when varying the temperature. We have explored the crossover regime where the adsorbed layers first begin to touch and interpenetrate ($h \sim h_c$). A sharp transition observed on the elastic part of the complex modulus $G^*(\omega)$ defines the crossover distance h_c with a very good accuracy (~5 Å).

Whatever the distance, the dynamic lubrication force, i.e., the hydrodynamic component of the complex modulus, varies continuously and the viscoelastic parameters—the zero-shear viscosity, the steady-state compliance, and the average relaxation time—account for the diffusion of solvent molecules and free chains. The enhancement of those quantities with confinement is due to the decreasing mesh size of the network created by the polymer layers related to the hydrodynamic correlation length ξ_H. The distance scaling predicted by Fredrickson and Pincus for moderately compressed layers, $\xi_H < h_0 < h_c$, is supposed to be independent of whether the layer is grafted or adsorbed to the surfaces. It rests on the assumption that the volume fraction of polymer in the layer is comparable to a semidilute solution. In good solvents, the scaling law $\xi_H \approx h_0^{3/4}$ is expected, and the prediction for Θ solvents is $\xi_H = h_0$. The experimental correlation we have found, $\xi_H \approx (h_c - h_0)^{-4/9}$, could be related to the weak-compression situation ($0.8 < h_0/h_c < 1$) whereas $\xi_H/h_c \approx 0.1$ allows us to explore more compressed regimes. Furthermore, Fredrickson and Pincus predict a complex modulus with an unusual scaling for the storage modulus in the low-frequency limit, $G_H'(\omega) \approx \omega^{13/11}$. Experimentally, the usual law, $G_H'(\omega) \approx \omega^2$, is verified and agrees with Sens' predictions[34] for adsorbed layers where the monomer concentration in the layers is assumed to vary as $C(z) \cong z^{-4/3}$. Sens attributes the anomalous behavior predicted by Fredrickson and Pincus to the fact that, for grafted polymer, the flow does not penetrate inside the polymer layer over the whole thickness but only over a size equal to the blob size ξ.

Another experimental finding is the elastic plateau modulus G_c emerging at low frequencies and for a well-defined distance h_c. That behavior is related to the direct interaction between the adsorbed layers, and h_c is a measure of the layer thickness.

Furthermore, there is a tight connection between the value of the plateau modulus G_c and the gradient of repulsive static forces. That is experimental evidence that the normal forces due to oscillatory compression of overlapped layers have the same origin as the static forces. A compression modulus $E_N(h_0)$ can be calculated from the measured modulus G_c. The values of E_N are between the rubbery and the glassy moduli of melts and suggest that the tethered chains have hindered motions when they are compressed and overlapped. At very low frequencies, relaxation processes similar to the tube retraction mechanism for branches of star polymers[35] could be exhibited by the loops and tails of adsorbed chains. At higher frequencies, the internal modes are excited and concern portions of chain of size ξ. This blob size is lower than the average distance between entanglements in a melt and suggests that the "semidilute solution" picture of the layers has to be revised.

In order to address the questions raised by the present work, experiments are in progress on well-defined systems. The main challenge is to identify and characterize the relaxation mechanisms within the layers, in both the compressed and uncompressed situations.

Acknowledgment. The authors thank J. F. Joanny for helpful suggestions. E.P. is grateful to the Conseil Régional d'Aquitaine for providing him with a research assistantship. This work has been sponsored by the CNRS in the framework of the GDR 936: "Mesures de forces de surface en milieu liquide".

References and Notes

(1) Ferry, J. D. *Viscoelastic Properties of Polymers*; John Wiley and Sons: New York, 1970.
(2) Israelachvili, J. N.; Tabor, D. *Proc. R. Soc. London* **1972**, *331*, 19.
(3) Chan, D. Y. C.; Horn, R. G. *J. Chem. Phys.* **1986**, *83*, 5311.
(4) Israelachvili, J. N. *J. Colloid Interface Sci.* **1986**, *110* (1), 263.
(5) Israelachvili, J. N.; Kott, S. J.; Fetters, L. *J. Polym. Sci. Part B* **1989**, *27*, 489.
(6) Israelachvili, J. N. *Colloid Polym. Sci.* **1986**, *264*, 1060.
(7) Montfort, J. P.; Hadzioannou, G. *J. Chem. Phys.* **1988**, *88* (11), 7187.
(8) Israelachvili, J. N. *Pure Appl. Chem.* **1988**, *60* (10), 1473.
(9) Klein, J.; Kamiyama, Y.; Yoshizawa, H.; Israelachvili, J. N.; Fredrickson, G. H.; Pincus, P.; Fetters, L. J. *Macromolecules* **1993**, *26*, 5552.
(10) Israelachvili, J. N.; McGuiggan, P. M.; Homola, A. M. *Science* **1988**, *240*, 189.
(11) Israelachvili, J. N.; Kott, S. J. *J. Colloid Interface Sci.* **1989**, *129* (2), 461.
(12) Homola, A. M.; Israelachvili, J. N.; Gee, M. L.; McGuiggan, P. M. *J. Tribol.* **1989**, *111*, 675.
(13) Van Alsten, J.; Granick, S. *Macromolecules* **1990**, *23*, 4856.
(14) Van Alsten, J.; Granick, S. *Langmuir* **1990**, *6*, 876.
(15) Granick, S. *Science* **1991**, *253*, 1374.
(16) Hu, H. W.; Granick, S. *Science* **1992**, *258*, 1339.

(17) Montfort, J. P.; Tonck, A.; Loubet, J. L.; Georges, J. M. *J. Polym. Sci., Part B* **1991**, *29*, 677.
(18) Tonck, A. Ph.D. Thesis Ecole Centrale de Lyon, N° 89−12, 1989.
(19) Georges, J. M.; Millot, S.; Loubet, J. L.; Tonck, A. *J. Chem. Phys.* **1993**, *98*, 7345.
(20) Ferry, J. D.; Berry, G. C.; Fox, T. G. *Adv. Polym. Sci.* **1968**, *5*, 261.
(21) Marin, G.; Menezes, E.; Raju, V. R.; Graessley, W. W. *Rheol. Acta* **1980**, *19*, 462.
(22) Struglinski, M. J. Ph.D. Thesis, Northwestern University, Evaston, IL, 1984.
(23) Brandrup, J.; Immergut, E. H. *Polymer Handbook*; Wiley: New York, 1975.
(24) Pelletier, E.; Montfort, J. P.; Loubet, J. L.; Tonck, A.; Georges, J. M., to be published.
(25) Thompson, P. A.; Robbins, M. O.; Grest, G. S. *Phys. Rev. Lett.* **1992**, *68*, 3448.
(26) de Gennes, P.-G. *Macromolecules* **1982**, *15*, 492.
(27) Fredrickson, G. H.; Pincus, P. *Langmuir* **1991**, *7*, 786.
(28) de Gennes, P.-G. *Scaling Concepts in Polymer Physics*; Cornell University Press: Ithaca, NY, 1979.
(29) Brochard-Wyart, F.; de Gennes, P.-G. *C. R. Acad. Sci. Paris* **1993**, *316*, 449.
(30) Rault, J. *C. R. Acad. Sci. Paris II* **1985**, *300*, 433.
(31) Montfort, J. P.; Marin, G.; Monge, P. *Macromolecules* **1986**, *19* (7), 393.
(32) Brochart-Wyart, F.; de Gennes, P.-G. *C. R. Acad. Sci. Paris II* **1993**, *316*, 449.
(33) de Gennes, P.-G. *C. R. Acad. Sci. Paris II* **1988**, *306*, 183.
(34) Sens, P.; Marques, C. M.; Joanny, J. F., submitted to *Macromolecules*.
(35) de Gennes, P.-G. *J. Phys. (Paris)* **1975**, *36*, 1199.

MA941266R